

Quantum Error Correction with Gauge Symmetries

Abhishek Rajput*

Department of Physics, University of Washington, Seattle, WA 98195, USA

Alessandro Roggero†

InQuBator for Quantum Simulation (IQuS), Department of Physics, University of Washington, Seattle, WA 98195, USA

Dipartimento di Fisica, University of Trento, via Sommarive 14, I-38123, Povo, Trento, Italy and

INFN-TIFPA Trento Institute of Fundamental Physics and Applications, Trento, Italy

Nathan Wiebe‡

Department of Computer Science, University of Toronto, Toronto, ON M5S 2E4, Canada

Pacific Northwest National Laboratory, Richland, WA 99354, USA and

Department of Physics, University of Washington, Seattle, WA 98195, USA

Quantum simulations of Lattice Gauge Theories (LGTs) are often formulated on an enlarged Hilbert space containing both physical and unphysical sectors in order to retain a local Hamiltonian. We provide simple fault-tolerant procedures that exploit such redundancy by combining a phase flip error correction code with the Gauss' law constraint to correct one-qubit errors for a \mathbb{Z}_2 or truncated U(1) LGT in 1+1 dimensions with a link flux cutoff of 1. Unlike existing work on detecting violations of Gauss' law, our circuits are fault tolerant and the overall error correction scheme outperforms a naïve application of the [5, 1, 3] code. The constructions outlined can be extended to LGT systems with larger cutoffs and may be of use in understanding how to hybridize error correction and quantum simulation for LGTs in higher space-time dimensions and with different symmetry groups.

I. INTRODUCTION

As gauge theories lie at the heart of the framework governing the interactions and forces described by the Standard Model, considerable effort has been expended in numerical simulations of these theories for computing physical quantities. Lattice gauge theories (LGTs) have been among the most fruitful formulations of non-perturbative approaches amenable for implementation on classical computers [1–5]. In regimes where classical simulations are plagued by an exponential scaling of the computational cost, digital quantum computers have emerged as a promising platform for the efficient simulation of LGTs. Notable examples are real-time dynamics or the study of systems at finite density [6–9].

Despite considerable advances on this front, digital quantum simulation of LGTs can time-evolve a given fiducial state into unphysical sectors due to noise and the approximation error associated with the simulation protocol used. A popular approach to mitigate this problem, especially useful for ground-state calculations but shown to be useful also out-of-equilibrium [10], is to enforce Gauss' Law by adding an energy penalty to the Hamiltonian (see e.g [6, 7, 10–12] and also [13] for techniques to reduce the gate cost of adding penalty terms). Another recent proposal for error mitigation in gauge theories uses random gauge transformations to suppress the component of the quantum state in the unphysical Hilbert space [14, 15]. The recent approach

proposed in [16], and its generalization to non-Abelian theories [17], uses instead a quantum oracle to detect the presence of gauge violating errors by performing explicit Gauss' Law checks and flagging an ancilla qubit. These techniques are suitable for error detection but in general do not possess error correction capabilities and are not fault-tolerant.

With the long-time goal of performing quantum simulation of LGT on fault-tolerant protocols, an intriguing possibility is to tailor general purpose error correction schemes to best exploit the structural properties of these theories in order to reduce the resource requirements for early explorations (see e.g. [18] for a recent attempt in this direction using the surface code). The physical intuition behind the approach followed in this work is that error correcting codes can be seen as artificial gauge theories where the logical Hilbert space is determined by states that satisfy a suitable local symmetry. When simulating LGTs which themselves need to satisfy a physical local symmetry, it might then be advantageous to exploit this natural redundancy to reduce the cost of the full error correction encoding.

We develop in this work fault-tolerant algorithms for error correction suitable for \mathbb{Z}_2 or truncated U(1) lattice gauge theories in 1+1 spacetime dimensions with a cutoff of 1 on the links. These algorithms combine the physicality constraint provided by Gauss' Law with bit and phase flip error correction codes [19] to detect and correct errors occurring on a site or the adjacent links. Error correction for a lattice with $2N$ links and $2N$ staggered fermionic sites with periodic boundary conditions is accomplished by tessellating these encodings across the whole lattice so that errors occurring on a particular site and its adjacent link can be detected by a Gauss' Law check on the next set of sites and links.

* rajpua@uw.edu

† a.roggero@unitn.it

‡ nawiebe@cs.toronto.edu

	Pure Gauge	Dynamical
[5,1,3]	10N	20N
Gauss' Law	9N	15N

TABLE I. Number of qubits required (excluding ancillas) for performing fault-tolerant error-correction with different encodings on a \mathbb{Z}_2 or truncated U(1) LGT system with $2N$ links, $2N$ staggered fermions, and a flux cutoff of 1. The case with non-dynamical fermions requires the same resources as the pure gauge case and is omitted from the table.

In the electric basis used here, a gauge violation is caused by bit-flip errors which can be corrected using a standard encoding based on the repetition code using $12N$ qubits: 3 for each site and 3 for each link (see the schematic illustration in Figure 1). The error correction procedure proposed here instead requires no bit-flip repetition code for the fermionic sites and a compressed encoding requiring only half of the qubits ($3N$ in total) for the link variables. Full fault-tolerance can then be achieved by concatenation with a standard phase-flip code (similar to what is done in the 9 qubit Shor code [19]) and using fault tolerant gadget design (e.g. using flag qubits [20]). For the simpler case when the fermionic sites are non dynamical, i.e. they can be represented by classical bits, the scheme proposed here requires $9N$ qubits for unit flux cutoffs with $O(1)$ ancillas. The full construction depicted in Figure 1 involving dynamical fermions requires $15N$ qubits with $O(1)$ ancillas. These are to be contrasted with the $10N$ and $20N$ qubits required for the two cases respectively using the [5,1,3] code for each site and link [21, 22]. It is foreseeable that more space efficient codes could be constructed, with the present work developing a first attempt to exploit the intrinsic redundancy present in gauge theories to reduce the cost of the error correction procedures required for their simulation at large scale.

The structure of the paper is as follows: Section II introduces the structure of U(1) and \mathbb{Z}_n Abelian LGTs. Section III surveys the basics of error correction codes and develops the formalism for integrating Gauss' law with a repetition code. Section IV then presents applications of these ideas for pure gauge theory first before treating the cases of error correction for an LGT with both non-dynamical and dynamical fermions. Section V summarizes the results and discusses future work for extending these results to different symmetry groups, and higher spacetime dimensions and flux cutoffs.

II. STRUCTURE OF U(1) AND \mathbb{Z}_n ABELIAN LATTICE GAUGE THEORIES

We follow the basic outline given in [16] and review the structure of abelian lattice gauge theories, specifically for the general gauge groups $G = \mathbb{Z}_n$ and $G = \text{U}(1)$ which contain those considered throughout this work. There are several physical models for which the gauge symmetries discussed here are important such as

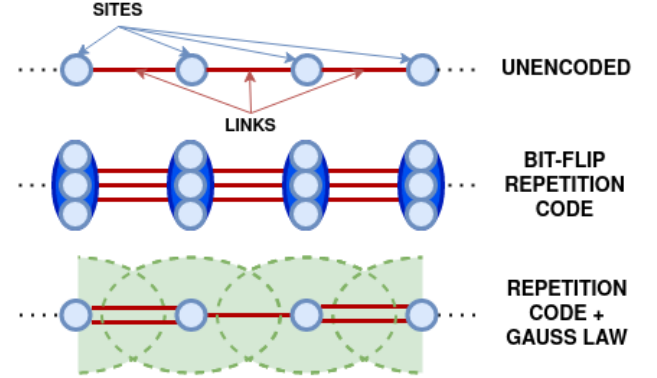


FIG. 1. Schematic illustration of the differences between two error correcting schemes for a simple one-dimensional LGT: a traditional bit-flip encoding scheme and the one proposed here exploiting the Gauss' Law gauge symmetry.

the Schwinger Model, or QED in 1+1 dimensions on a lattice [23, 24]. It is the one of the simplest concrete examples of an Abelian LGT and serves as a convenient setting for the analysis and application of Gauss' Law symmetries to error correction. This model has been extensively used as an important stepping stone in simulations of lattice field theories using both tensor networks and quantum devices [11, 25–28].

We discretize space on a cubic lattice L with sites labeled by s and links labeled by l . We assume that the lattice consists of N sites for even $N \geq 0$ and that a staggered fermion representation is used wherein every second site is positronic. Each link l is associated an independent separable Hilbert space \mathcal{H}_l with the same orthonormal basis:

$$\langle m' | m \rangle = \delta_{m',m}, \quad \hat{1} = \sum_m |m\rangle \langle m| \quad (1)$$

with

$$m', m \in \begin{cases} \mathbb{Z}_n, & \text{if } G = \mathbb{Z}_n \\ \mathbb{Z}, & \text{if } G = \text{U}(1). \end{cases}$$

The Hamiltonian for this LGT is a function of the link operators \hat{U}_l and their conjugate electric fields \hat{E}_l defined explicitly in this basis by

$$\hat{U}_l = \sum_{m_l} |m+1\rangle \langle m|, \quad \hat{E}_l = \sum_{m_l} m_l |m_l\rangle \langle m_l|. \quad (2)$$

From this expression we can see that \hat{U}_l acts as a raising operator and its adjoint as a lowering operator on the Hilbert space \mathcal{H}_l of the link. Operators defined on different link Hilbert spaces commute while the same-link commutation relations are given by

$$[\hat{E}_l, \hat{U}_l] = \hat{U}_l, \quad G = \text{U}(1) \quad (3)$$

$$Q_l \hat{U}_l \hat{Q}_l^\dagger = \hat{U}_l e^{2\pi i / n} \quad G = \mathbb{Z}_n \quad (4)$$

where

$$\hat{Q}_l := e^{2\pi i \hat{E}_l / n} = \sum_{m_l=0}^{N-1} e^{2\pi i m_l / n} |m_l\rangle \langle m_l|.$$

The form of the commutation relation for \mathbb{Z}_n is due to the fact that the electric field values are periodic, so the Hamiltonian depends on \hat{Q}_l .

When considering fermionic matter fields on the sites, we work in the occupation number basis where number operators n_σ are diagonal with eigenvalues $\{0, 1\}$. Here, σ is a collective index denoting the relevant species or indices (like flavor or spinor) involved. The global state of the entire lattice is spanned by a basis given by a specification of electric fields on the links of the lattice and occupation numbers on the sites. Due to the locality of the symmetry, we will typically consider a particular site on a lattice and those links attached to it and denote the corresponding basis states by

$$|\mathbf{E}, \rho\rangle \rightarrow \otimes_{i=1}^D |E_i(s)\rangle \otimes_{i=1}^D |E_i(s - \hat{e}_i)\rangle \otimes_\sigma |n_\sigma\rangle,$$

where D is the spatial dimension of the lattice.

Due to gauge invariance, states in the physical Hilbert space satisfy a local Gauss' Law which relates the state of a site with the state of the links emanating from it. Gauge-invariant states are in the kernel of the operator

$$\begin{aligned} \hat{G}_s &:= (\nabla \cdot \hat{E})(s) - \hat{\rho}(s) \\ &:= \sum_{i=1}^D (\hat{E}_i(s) - \hat{E}_i(s - \hat{e}_i)) - \sum_\sigma e_\sigma \hat{n}_\sigma(s), \end{aligned} \quad (5)$$

where $e_\sigma = \pm 1$ and the second line is obtained by discretization of the gradient operator on the lattice.

When dealing with a U(1) gauge group, it is necessary to truncate the link electric field values to enable digital quantum simulation with a finite number of qubits. This can be accomplished by "wrapping" the electric field at a cutoff Λ :

$$E_l = \sum_{\epsilon=-\Lambda}^{\Lambda-1} \epsilon |\epsilon\rangle_l \langle \epsilon|_l \quad (6)$$

$$U_l |\Lambda - 1\rangle_l = |-\Lambda\rangle_l \quad (7)$$

$$U_l^\dagger |-\Lambda\rangle_l = |\Lambda - 1\rangle_l. \quad (8)$$

This choice of discretization results in a modification of the commutation relations as follows:

$$[E_l, U_l] = U_l - 2\Lambda |-\Lambda\rangle_l \langle \Lambda - 1|_l \quad (9)$$

$$[E_l, U_l^\dagger] = -U_l^\dagger + 2\Lambda |\Lambda - 1\rangle_l \langle -\Lambda|_l. \quad (10)$$

Note that with our choice of the lower and upper bound, the link Hilbert spaces are even-dimensional and can therefore be mapped onto a $\lceil \log(2\Lambda) \rceil$ -qubit Hilbert space. In this work, we will restrict the discussion to $\Lambda = 1$ and comment on the prospects of generalizing our constructions to arbitrary cutoffs in [Section V](#).

III. ERROR CORRECTION WITH GAUSS' LAW

We now briefly discuss the bit and phase-flip error correction codes used throughout the paper and show how to integrate them with Gauss Law to reduce the number of qubits required. The overarching idea is to perform an encoding of the link physical qubits into logical states and use the local gauge symmetry to implement a more space efficient error correction code under an error model with arbitrary single-qubit errors.

A. Preliminaries on the repetition code

We outline in this section the basics of the bit and phase flip error correction codes following the treatment given in [\[29\]](#). First consider a noisy classical communications channel through which we wish to send a bit between two locations and suppose its behavior is such that it flips the bit with probability p . To protect the bit against the effects of noise, we can employ what is known as a "repetition code". This involves replacing the bit with three copies of itself, i.e. $0 \rightarrow 000$ and $1 \rightarrow 111$. These new bit strings are denoted as the "logical 0" and "logical 1" and we send these through the channel. The receiver then attempts to decode what the original bit was. If the output is 010 for instance, then provided the probability p of error is not high and the noise acts independently on each bit, it is likely the second bit was flipped and that the original bit was 0. This is known as majority voting, since the intended original message is determined by whatever bit value appears more in the output. This can obviously fail if more than one bit was flipped. It can be easily determined that with this encoding scheme, the transmission becomes more reliable if $p < 1/2$.

Now consider a noisy quantum channel that applies a bit-flip, or X gate, to a state $|\psi\rangle$ sent through it with probability p . We write $|\psi\rangle$ in terms of the computational basis as $|\psi\rangle = a|0\rangle + b|1\rangle$ and encode it in three qubits as $a|000\rangle + b|111\rangle$. In other words, we have a mapping between the "physical" qubits $|0\rangle$ and $|1\rangle$ to the logical qubits $|0\rangle_L = |000\rangle$ and $|1\rangle_L = |111\rangle$ respectively, where the subscript L denotes a logical state. Such an encoding can be accomplished by the circuit in [Figure 2](#).

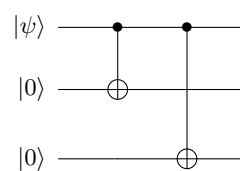


FIG. 2. Circuit for creating the encoded logical state $|\psi\rangle_L = a|000\rangle + b|111\rangle$ for the bit-flip code.

Z_1Z_2	Z_2Z_3	Correction
1	1	III
1	-1	IIX
-1	1	XII
-1	-1	IXI

TABLE II. Syndrome measurements outcomes, and correction operations for bit flip error correction code.

Each qubit in the encoded state is passed through a separate bit-flip channel. If a bit-flip occurs on at most one qubit, we can measure the parities of the qubits by performing projective measurements of the operators Z_1Z_2 and Z_2Z_3 , where the tensor product is implied. This process is known as making “syndrome measurements” for the error syndromes Z_1Z_2 and Z_2Z_3 . These operators have eigenvalues of ± 1 . Z_1Z_2 measures the parities of the first two qubits and yields the eigenvalue -1 if they differ and $+1$ if they do not. Z_2Z_3 acts in the same way for the second and third qubits. The measurement outcomes of either operator allows us to determine which qubit was flipped. For instance, if eigenvalues of -1 are obtained from the measurement of both operators, we know that with high probability the second qubit was flipped. We can then perform error correction by applying an X gate on the 2nd qubit to flip it back to its original state. Note that the measurement of these operators gives no information about the amplitudes a and b of the encoded state and therefore do not destroy the state we wish to perform error detection and correction on. [Table II](#) outlines the possible measurement outcomes for the syndromes Z_1Z_2 and Z_2Z_3 and the error correction operations to perform. [Figure 3](#) gives the full circuit to correct bit-flip errors. An equivalent circuit used for the projective measurement of the stabilizers Z_1Z_2 and Z_2Z_3 is presented in [Figure 4](#). We will use this decomposition in the rest of this work.

Now suppose we have a noisy quantum channel that applies a phase flip (i.e a Z gate) with probability p to a qubit in the state $|\psi\rangle = a|0\rangle + b|1\rangle$. Unlike the bit-flip encoding, there is no classical analogue of applying a “phase” to a bit. However, we can convert

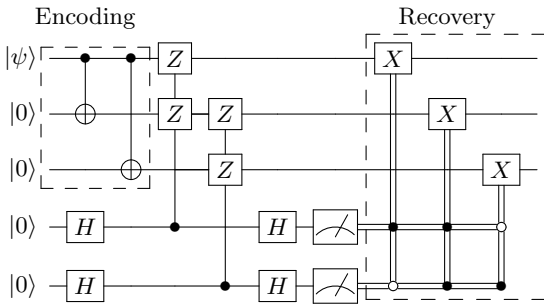


FIG. 3. Full circuit for correcting a bit flip errors on a general state $|\psi\rangle$.

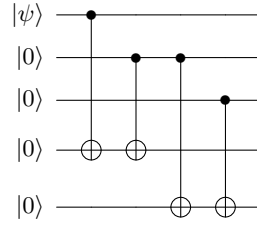


FIG. 4. Equivalent circuit for the measurement of the stabilizers Z_1Z_2 and Z_2Z_3 for the bit-flip error correction code. This can be obtained from the identity $HZH = X$ and the fact that controlled-Z gates are equivalent to a controlled-Z gate with the control and target flipped.

this channel to a bit flip channel by working in the $|+\rangle = (|0\rangle + |1\rangle)/\sqrt{2}$ and $|-\rangle = (|0\rangle - |1\rangle)/\sqrt{2}$ basis. With respect to this basis, the Z operator takes $|+\rangle$ to $|-\rangle$ and therefore acts as a bit flip. We can then apply the same logic for error correction in the bit-flip case to the present case by switching from the computational basis to the $|+\rangle$ and $|-\rangle$ basis via the Hadamard gate. In our present work, we will find it convenient to use the logical codeword basis $|0\rangle_L = (|+++| - |---|)/\sqrt{2}$ and $|1\rangle_L = (|+++| + |---|)/\sqrt{2}$. Then to detect errors, we can perform projective measurements of the stabilizers X_1X_2 and X_2X_3 to determine the parity of the bits. Based on the measurement outcomes, we can apply Z gates to correct the errors accordingly. The encoding circuit and the phase-flip error correction procedure are depicted in [Figure 5](#) and [Figure 6](#) respectively.

The constructions given in [\[20\]](#) allow us to ensure the fault tolerance of the encoding, error detection, and recovery operations in either code. The underlying technique involves introducing an extra “flag” qubit prepared in the $|+\rangle$ state and performing CNOT operations from it on the syndrome ancilla qubit at key points in the circuit (see Figure 3(b) in [\[20\]](#)). This flag qubit is then measured in the X basis and a result of $|-\rangle$ indicates an error of weight two or more on the data qubits. Additional flag qubits can be added between each gate in the stabilizer measurement to ensure a localization of errors. Similar constructions apply in creating fault-tolerant versions of other important subroutines like log-

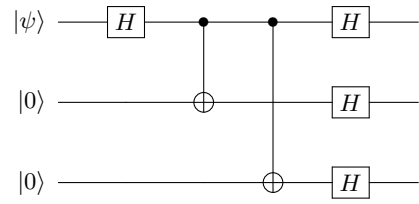


FIG. 5. Circuit for creating the encoded logical state $|\psi\rangle_L = a|0\rangle_L + b|1\rangle_L$ for the phase-flip code, where $|0\rangle_L = (|+++| - |---|)/\sqrt{2}$ and $|1\rangle_L = (|+++| + |---|)/\sqrt{2}$.

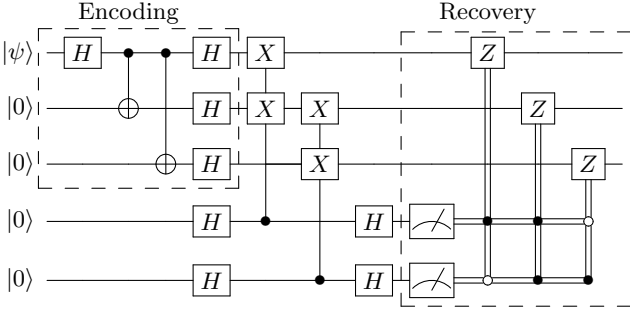


FIG. 6. Full circuit for correcting phase flip errors on a general state $|\psi\rangle$.

ical state-preparation and stabilizer measurements (see Appendix A in [20]).

B. Integrating the repetition code with Gauss' Law

We are now in the position to discuss how the expression of Gauss' Law in Eq. (5) can remove the need to use an explicit bit flip code in fault tolerant LGT simulations. To simplify the discussion we will henceforth consider the one dimensional case ($D = 1$) with staggered fermionic sites, where only one fermionic flavor with charge e_s is present on any given site s . The Gauss' Law operator at site s between links l and $l + 1$ simplifies then to

$$\hat{G}_s = \hat{E}_{l+1} - \hat{E}_l - e_s \hat{n}(s) , \quad (11)$$

and in the simpler pure gauge case with no matter to

$$\hat{G}_s = \hat{E}_{l+1} - \hat{E}_l . \quad (12)$$

We start by discussing the latter case and consider a general state of the two links in the electric basis

$$|\Psi_{l,l+1}\rangle = \sum_{\epsilon_l} \sum_{\epsilon_{l+1}} \Psi_{\epsilon_l, \epsilon_{l+1}} |\epsilon_l\rangle \otimes |\epsilon_{l+1}\rangle . \quad (13)$$

Following the discussion in Sec. II, a physical state needs to be in the kernel of the Gauss' Law operator. Using Eq. (12) above we see that \hat{G}_s acts on $|\Psi_{l,l+1}\rangle$ as

$$\hat{G}_s |\Psi_{l,l+1}\rangle = \sum_{\epsilon_l} \sum_{\epsilon_{l+1}} \Psi_{\epsilon_l, \epsilon_{l+1}} (\epsilon_{l+1} - \epsilon_l) |\epsilon_l\rangle \otimes |\epsilon_{l+1}\rangle , \quad (14)$$

and is zero only if the coefficient matrix is diagonal

$$\Psi_{\epsilon_l, \epsilon_{l+1}}(\epsilon_{l+1} - \epsilon_l) = 0 \Leftrightarrow \Psi_{\epsilon_l, \epsilon_{l+1}} = \Psi_{\epsilon_l} \delta_{\epsilon_l, \epsilon_{l+1}}. \quad (15)$$

This argument, which can be easily generalized to the case where the state of the links is mixed, shows that gauge invariant states are analogous to a bit-flip repetition code with only two copies: $|0\rangle_L = |0\rangle \otimes |0\rangle$ and

$|1\rangle_L = |1\rangle \otimes |1\rangle$. The distance between these codewords is not sufficient to allow for error correction but is sufficient for error detection (see e.g. [30]). This explains in an intuitive way why oracles like those presented in Ref. [16] are capable of detecting bit-flip errors without requiring additional qubits for the encoding.

It is now easy to see how the use of Gauss' Law allows for a space reduction in the bit-flip encoding: the standard procedure described above will require three link registers to encode a logical link as

$$\begin{aligned} |\Phi_l\rangle_L &\coloneqq \sum_{\epsilon_l} \Phi_{\epsilon_l} |\epsilon_l\rangle \otimes |\epsilon_l\rangle \otimes |\epsilon_l\rangle \\ &= \sum_{\epsilon_l} \Phi_{\epsilon_l} |\epsilon_l\rangle_L. \end{aligned} \quad (16)$$

The fact that physical states satisfy Eq. (14) means we need only two registers per link and can use one of the two registers for the $l + 1$ link across a site s when we measure stabilizers and perform error recovery. Since only three registers are involved in this procedure, we will consider a construction with two qubit registers for even links and only one register for the odd links in order to minimize the memory cost. More explicitly, we will use the alternative encoding

$$|\Phi_l\rangle_{GLE} \coloneqq \sum_{\epsilon_l} \Phi_{\epsilon_l} |\epsilon_l\rangle \otimes |\epsilon_l\rangle = \sum_{\epsilon_l} \Phi_{\epsilon_l} |\epsilon_l\rangle_{GLE} , \quad (17)$$

for the even links in the lattice and

$$|\Phi_l\rangle_{GLO} \coloneqq \sum_{\epsilon_l} \Phi_{\epsilon_l} |\epsilon_l\rangle = \sum_{\epsilon_l} \Phi_{\epsilon_l} |\epsilon_l\rangle_{GLO} , \quad (18)$$

equivalent to a bare encoding, for the odd links. For physical states that satisfy the Gauss' law constraint in Eq. (15) we have then

$$\begin{aligned}
|\Phi_{l,l+1}\rangle_{GL} &= \sum_{\epsilon_l} \sum_{\epsilon_{l+1}} \Psi_{\epsilon_l, \epsilon_{l+1}} |\epsilon_l\rangle_{GLE} \otimes |\epsilon_{l+1}\rangle_{GLO} \\
&= \sum_{\epsilon_l} \Psi_{\epsilon_l} |\epsilon_l\rangle_{GLE} \otimes |\epsilon_l\rangle_{GLO} \\
&= \sum_{\epsilon_l} \Psi_{\epsilon_l} |\epsilon_l\rangle \otimes |\epsilon_l\rangle \otimes |\epsilon_l\rangle ,
\end{aligned} \tag{19}$$

and we can now use the stabilizer measurements and recovery operation on the three qubits as in the bit-flip repetition code. The second line is obtained by ensuring that the logical state $|\Phi_{l,l+1}\rangle_{GL}$ is in the kernel of the logical Gauss Law operator derived from Eq. (12)

$$\begin{aligned}\hat{G}_s^{(GL)} &= \hat{E}_{l+1}^{(GLO)} - \hat{E}_l^{(GLE)} \\ &= \hat{E}_{l+1} - \hat{E}_l \otimes \hat{E}_l.\end{aligned}\tag{20}$$

The expressions above apply directly to sites s between l even and $l+1$ odd, but it is straightforward to generalize them to the site $s+1$ where the left link is odd and the

right link is even as follows

$$\begin{aligned}
|\Phi_{l+1,l+2}\rangle_{GL} &= \sum_{\epsilon_{l+1}} \sum_{\epsilon_{l+2}} \Psi_{\epsilon_{l+1},\epsilon_{l+2}} |\epsilon_{l+1}\rangle_{GLO} \otimes |\epsilon_{l+2}\rangle_{GLE} \\
&= \sum_{\epsilon_{l+1}} \Psi_{\epsilon_{l+1}} |\epsilon_{l+1}\rangle_{GLO} \otimes |\epsilon_{l+1}\rangle_{GLE} \\
&= \sum_{\epsilon_{l+1}} \Psi_{\epsilon_{l+1}} |\epsilon_{l+1}\rangle \otimes |\epsilon_{l+1}\rangle \otimes |\epsilon_{l+1}\rangle. \quad (21)
\end{aligned}$$

The gauge invariant logical state is again equivalent to the standard bit-flip encoding shown in Eq. (16). Since Gauss' Law only detects errors in the flux value, which in our representation corresponds to bit-flip errors, each register of qubits in the construction presented above needs to be encoded in a phase-flip code to ensure that all single errors are correctable. With this concatenation, the gauge-invariant logical states $|\Phi_{l,l+1}\rangle_{GL}$ and $|\Phi_{l+1,l+2}\rangle_{GL}$ become equivalent to a full 9-qubit encoding [19]. However, we encode two full links using the 9-qubit encoding as opposed to each link separately. This encoding therefore has better memory efficiency than error correcting codes that act on individual qubits, the best one requiring 5 qubits [21, 22]. Note that it is still possible to find codes with even higher memory efficiency when multiple logical qubit are encoded. For instance, 3 logical qubits can be encoded into 8 while correcting all single errors (see eg. [31, 32]).

Adding fermions to the system modifies the relation between link states across a site so that they do not necessarily need to be the same. The full state around a site s is a generalization of Eq. (13) and should now be written as

$$|\Psi_{l,l+1}^s\rangle = \sum_{\epsilon_l} \sum_{\epsilon_{l+1}} \sum_{n=0,1} \Psi_{\epsilon_l, \epsilon_{l+1}}^n |\epsilon_l\rangle \otimes |\epsilon_{l+1}\rangle \otimes |n\rangle_s. \quad (22)$$

The gauge-invariance constraint becomes therefore

$$\begin{aligned}
\Psi_{\epsilon_l, \epsilon_{l+1}}^0 (\epsilon_{l+1} - \epsilon_l) &= 0, \\
\Psi_{\epsilon_l, \epsilon_{l+1}}^1 (\epsilon_{l+1} - \epsilon_l - e_s) &= 0. \quad (23)
\end{aligned}$$

A state belonging to the physically meaningful portion of the Hilbert space is then

$$|\Psi_{l,l+1}^s\rangle = \sum_{\epsilon_l} \sum_{n=0,1} \Psi_{\epsilon_l}^n |\epsilon_l\rangle \otimes |\epsilon_l + ne_s\rangle \otimes |n\rangle_s, \quad (24)$$

where we recall that $e_s = 1$ for a fermionic site and $e_s = -1$ for an anti-fermionic site. In order to obtain a useful encoded state for error correction, we can then apply a lowering operator \hat{U}_{l+1}^\dagger (for $e_s = 1$) or a raising operator \hat{U}_{l+1} (for $e_s = -1$) to the link $l+1$ controlled on the state of the site qubit. Calling this operation \hat{W}_s , for a site between an even and an odd link we have that

$$\begin{aligned}
\hat{W}_s |\Psi_{l,l+1}^s\rangle_{GL} &= \sum_{\epsilon_l} \sum_{n=0,1} \Psi_{\epsilon_l}^n |\epsilon_l\rangle_{GLE} \otimes |\epsilon_l\rangle_{GLO} \otimes |n\rangle_s \\
&= \sum_{\epsilon_l} \sum_{n=0,1} \Psi_{\epsilon_l}^n |\epsilon_l\rangle \otimes |\epsilon_l\rangle \otimes |\epsilon_l\rangle \otimes |n\rangle_s \quad (25)
\end{aligned}$$

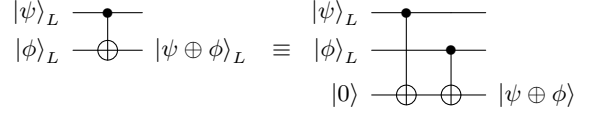


FIG. 7. Equivalence for logical CNOT between logical qubits and for two logical-to-physical CNOTs.

and the error correction procedure can be carried out on this new state. After one site has been processed, we apply the inverse \hat{W}_s^\dagger and move to the next site. In this approach, we effectively move from a gauge-invariant encoding that satisfies Eq. (23) to a logical encoding equivalent to the bit-flip code by using \hat{W}_s and its inverse. This operation needs to be performed fault-tolerantly in order to ensure a controlled propagation of errors. In the next section we will restrict the discussion to the simpler case where the link registers are formed by a single qubit (ie. the flux cutoff is set to one). In that case, we show that the construction can be done in a fault-tolerant way.

It is preferable to avoid directly implementing the \hat{W}_s operation in practice as bit-flip errors can propagate from the site used as the control for the $l+1$ link. This can be done by adopting a full bit-flip encoding for the site alone and using the measurement of its stabilizers to correct for the induced error in the link. A more efficient strategy however is to compute the parity between the $l+1$ link and the adjacent site and store the result in a physical ancilla qubit, as shown schematically in Figure 7. The ancilla qubit can then be used as part of a logical encoding for the even-numbered links. We can catch errors of weight two or higher that occur from errors propagating past the logical CNOTs with the use of flag qubits (see [20]) and an example of this is shown in Figure 9. This construction can be readily extended to situations with large cutoffs if we employ a unary encoding for the flux state using m qubits per link, in which case we will require m ancilla qubits. Generalizing the approach to larger cutoff values with various encodings is an important issue which will need to be addressed in future work (see also Sec. V). As we show in more detail in the next section, using ancilla qubits to temporarily store the parity of the two links allows for a fault-tolerant error correction of a gauge theory with dynamical fermions using the unencoded sites directly, providing a significant saving in qubits.

In summary, the number of link registers required for the Gauss' Law aided bit-flip error correction is $3N$ for a system with a total of $2N$ links. The total number of qubits required in a pure gauge simulation is therefore $9N + O(1)$ when restricting the unit electric cutoff case as done above and accounting for the additional 3 physical qubits required for the phase-flip encoding. With the addition of dynamical fermions on $2N$ sites, one can exploit the relationship given by Gauss' law between the state of a site and its adjacent links to do

error correction with a total of $15N + O(1)$ qubits, $9N$ for links and $6N$ for sites. These are impossible results if one instead attempts to perform error correction on individual qubits. The total space required would instead be $10N$ for the non-dynamical case and $20N$ for the dynamical one using the perfect 5-qubit encoding from [21, 22]. As mentioned previously, better ratios are possible if one encodes multiple logical qubits at a time and we leave the extension to the more efficient encodings for future work [31, 32].

IV. APPLICATIONS

We hereafter specialize to a \mathbb{Z}_2 or truncated $U(1)$ gauge theory in 1+1 dimensions with a cutoff of $\Lambda = 1$ for the flux in each link. We work with a system with $2N$ sites and $2N$ links with PBCs. Site k , for an integer $k \geq 1$, is denoted by S_k^1 and the links coming into and out of the site are written as L_k^1 and L_{k+1}^1 respectively.

Unless otherwise specified, every circuit in this section is a concatenated one, with every qubit encoded within the phase flip error-correcting code as in Figure 5. Logical qubits arising in this manner will be denoted with the subscript L .

This section presents applications of the previous analysis to a few gauge theories in order of increasing generality. Beginning with the pure gauge theory case with no matter present on the sites, Gauss' Law gives the equality between the incoming and outgoing flux on a site. This allows us to use $|L_k^1\rangle$ and $|L_{k+1}^1\rangle$ as part of a single logical qubit for a concatenated bit-flip error correction procedure, where an additional qubit is introduced only if the links are even-numbered.

This situation is easily generalized to a theory with static charges or non-dynamical fermions on the sites by applying a link lowering operator on an odd-numbered link conditioned on the classical state of the adjacent site. We then perform the error correction procedure on the appropriate logical link qubit before restoring the odd link's flux value with a raising operator.

The scenario with dynamical fermions is dealt with by computing the parity between an odd-numbered link and its adjacent site and storing the result in a physical ancilla qubit. This qubit is then used as part of a logical encoding for the even-numbered links. Bit-flip checks can be performed on two sets of adjacent links and sites and the information from them can be used to correct errors on all the relevant qubits, provided there is a single bit-flip error per two such checks.

Note that we cannot perform this analysis entirely within the stabilizer formalism since our controlled operations are not logical ones at the level of the bit-flip encoding. While certain aspects of our treatment therefore rely on standard constructions within the stabilizer formalism, others involving Gauss' Law require us to move between physical and logical states.

Pure Gauge Theory

We adopt the notation $|L_k^n\rangle_L$ and $|S_k^n\rangle_L$ to denote link and site logical qubits respectively in the phase flip code, and O_k^n for operators acting on the k -th logical link or site qubit. The case where $n = 1$ in the superscript denotes the original logical qubit and logical qubit operator, while values of n greater than 1 denote the auxiliary link or site qubits introduced for the error correction procedures. If a given logical site or link is the only one of its kind, we will drop the superscript.

In each of the subsequent circuits, we introduce no additional qubits for the odd numbered links and an auxiliary qubit $|L_{2k}^2\rangle_L$ for each even numbered link $|L_{2k}^1\rangle_L$ that is arranged to have the same state as $|L_{2k}^1\rangle_L$. The constraint that the fluxes satisfy Gauss' Law at site $|S_{2k}^1\rangle_L$ with associated link qubits $\{|L_{2k}^1\rangle_L, |L_{2k}^2\rangle_L, |L_{2k+1}^1\rangle_L\}$ will then ensure that $|L_{2k}^1\rangle_L = |L_{2k}^2\rangle_L = |L_{2k+1}^1\rangle_L$, or more precisely that the wave-function factorizes as in Eq. (19) above.

As noted in the previous section, the grouping $\{|L_{2k}^1\rangle_L, |L_{2k}^2\rangle_L, |L_{2k+1}^1\rangle_L\}$ acts as a 3-qubit logical encoding for the link logical qubit $|L_{2k}^1\rangle_L$ that can be used in the bit flip error correction code outlined in Figure 8. The circuit is however sensitive to single qubit phase flip errors that propagate to weight two or three phase flip errors. This is due to the use of logical to physical CNOT gates, which enable the propagation of physical Z errors from the target of these CNOTs to logical Z errors on the links. We therefore employ the fault-tolerant logical-to-physical CNOT depicted in Figure 9. This CNOT is implicitly used in all the subsequent circuits where logical-to-physical CNOT operations occur.

Non-Dynamical Fermions

It is straightforward to generalize the results of the preceding subsection to the case where we have non-dynamical fermions on the sites. Since we know in this

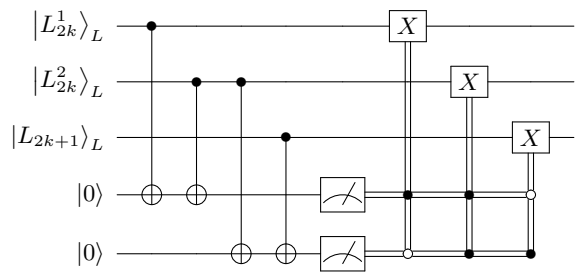


FIG. 8. Bit-flip syndrome measurement and correction operations for links. The subscript L denotes the phase-flip encoding of these qubits shown in Figure 5. Each CNOT operation here consists of three individual CNOTs from the qubits in the underlying phase-flip encoding. Here X is the operation $X \otimes X \otimes X$ which acts as a logical X .

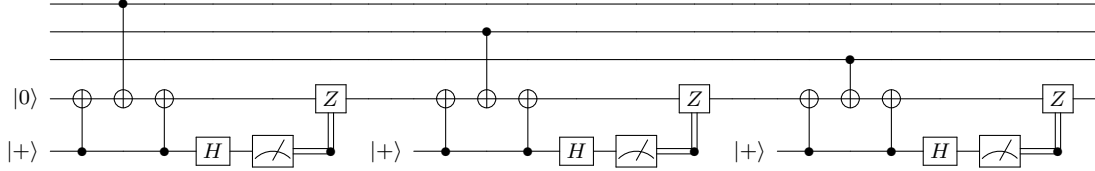


FIG. 9. Fault tolerant logical-to-physical CNOT using flag qubits.

case whether or not a certain physical site S_{2k} (this is not a logical site qubit but a classical binary variable) has a fermion, it is not necessary to introduce an ancilla qubit and use the equivalence in Figure 7. The controlled operation \hat{W}_s introduced above (see Eq. (25)) is instead replaced by its classically controlled counterpart. As such, we apply a classically conditioned link-lowering operator to $|L_{2k+1}\rangle_L$ to “lower” its flux value and have it match that of $|L_{2k}^1\rangle_L$. We then apply the preceding bit-flip error correction code and restore the flux value of $|L_{2k+1}^1\rangle_L$ back to its original value with a classically conditioned link-raising operation.

Given our assumptions on the flux cutoff, we have the circuit in Figure 10 for the non-dynamical fermionic case. This construction also holds for an arbitrary site S_k and not just even numbered ones.

Dynamical Fermions

A naïve approach to extend the preceding constructions to the case with dynamical staggered fermions on the sites is to apply a CNOT gate to $|L_{2k+1}\rangle_L$ conditioned on the state of $|S_{2k}\rangle_L$. We could then introduce additional qubits $|S_{2k}^2\rangle_L$ and $|S_{2k}^3\rangle_L$ to create a bit-flip encoding of $|S_{2k}\rangle_L$ and thereby protect it from bit-flip errors. Errors propagating to $|L_{2k+1}\rangle_L$, $|L_{2k}^1\rangle_L$, and $|L_{2k}^2\rangle_L$ can be corrected with a separate bit-flip code involving these qubits, with additional recovery operations included to account for the propagation of X errors past the control of the CNOT.

This construction only involves Clifford operations

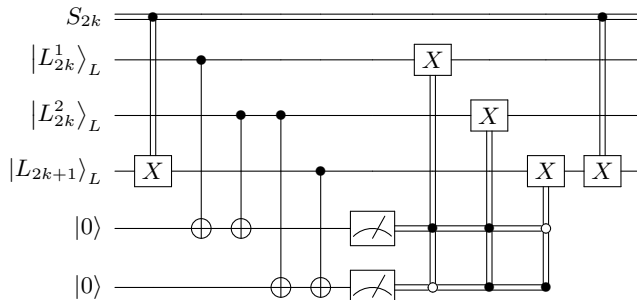


FIG. 10. Syndrome measurement and correction operations for LGT system with non-dynamical fermions. The circuit holds for arbitrary sites S_k and not just even numbered ones.

and can easily be made fault tolerant. It however requires $18N + 6N + 3N = 27N$ qubits for an $2N$ site and $2N$ link system excluding ancillas, which is suboptimal compared to the $20N$ qubits obtained from using the $[5, 1, 3]$ encoding for each site and link.

We instead develop a procedure that further exploits Gauss’ law to reduce the cost to $15N$ qubits. This is achieved by noticing that, as discussed in Sec. III B, given the state on a site S_{2k+1} and its adjacent links L_{2k+1} and L_{2k+2} , a bit-flip error on any of these qubits will cause a violation of Gauss’ law. The ambiguity in where the error occurred can be resolved by overlapping Gauss’ law checks on the preceding and subsequent site and their adjacent links. In fact, we will show only two such checks are needed to resolve the ambiguity.

Figure 11 depicts to overlapping Gauss’ law checks \mathcal{G}_{2k} and \mathcal{G}_{2k+1} on sites S_{2k} and S_{2k+1} respectively. Consider \mathcal{G}_{2k+1} in particular. We can compute the parity between $|S_{2k+1}\rangle_L$ and $|L_{2k+1}\rangle_L$ as per Figure 7 and store this result into a physical ancilla qubit $|0\rangle$, which serves as a proxy for $|L_{2k+1}\rangle_L$ but with its flux value reset. We can then treat $|0\rangle$, $|L_{2k+2}^1\rangle_L$, $|L_{2k+2}^2\rangle_L$ as a logical qubit for a bit-flip error correction code and uncompute the value in $|0\rangle$ afterwards. These steps constitute \mathcal{G}_{2k+1} for the odd sites and their neighboring links and are repeated analogously across the lattice.

To see how the information obtained from the stabilizer measurements employing the last two ancilla qubits in Figure 11 helps us correct errors on the data qubits, consider \mathcal{G}_{2k+1} first. The syndrome measurement outcomes 10 and 01 uniquely identify bit-flip errors occurring on the even links $|L_{2k+2}^1\rangle_L$ and $|L_{2k+2}^2\rangle_L$ respectively. The remaining non-trivial outcome 11 indicates a bit-flip error on either $|L_{2k+1}\rangle_L$ or $|S_{2k+1}\rangle_L$ with no way to resolve the ambiguity.

If the error occurred on $|S_{2k+1}\rangle_L$ however, we would obtain the syndrome 00 from the check \mathcal{G}_{2k} as Gauss’ law is satisfied between S_{2k} , L_{2k} , and L_{2k+1} . If the error occurred on $|L_{2k+1}\rangle_L$, we would then obtain the syndrome 11 from \mathcal{G}_{2k} . As these two cases yield distinct syndromes, we can resolve the aforementioned ambiguity as shown in Table III. Note that this analysis will only hold if a bit-flip error occurs once during the checks \mathcal{G}_{2k} and \mathcal{G}_{2k+1} .

To assess the fault-tolerance of this construction, we first consider the possibility that single-qubit bit flip errors occurring at the physical level can propagate to undetectable errors at level of the phase-flip code. Con-

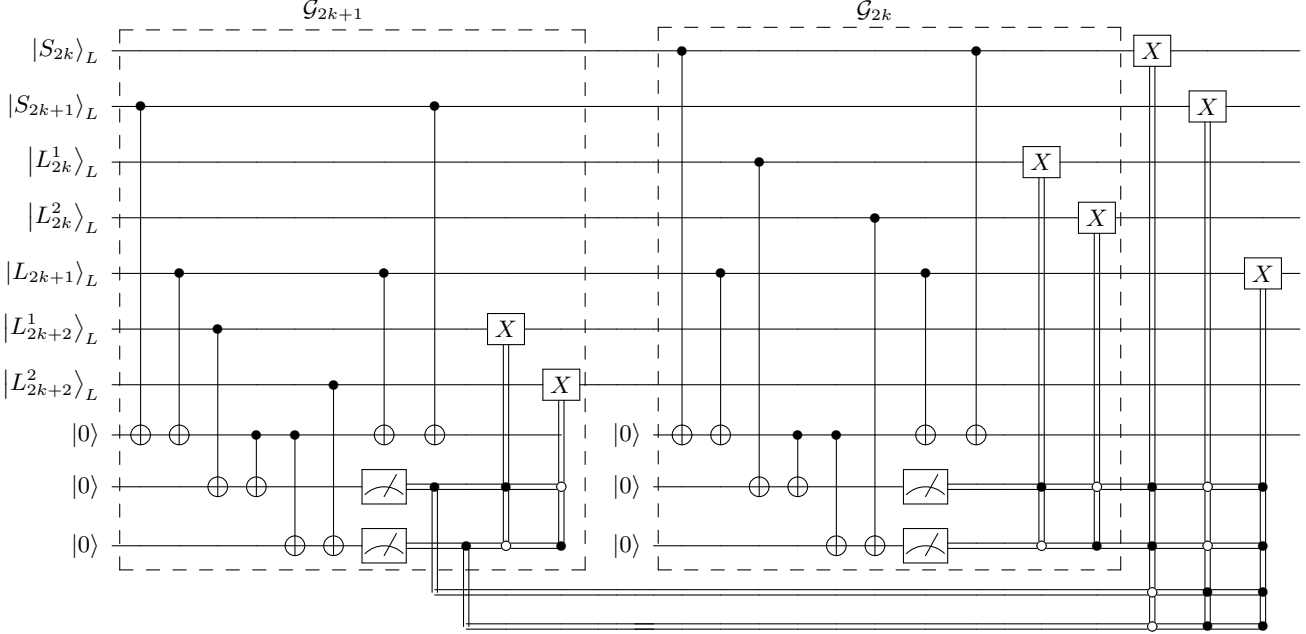


FIG. 11. Circuit for using information from Gauss' Law checks \mathcal{G}_{2k} and \mathcal{G}_{2k+1} on S_{2k} , S_{2k+1} , and their adjacent links to correct bit-flip errors on them. Bit-flip errors on even-numbered links can be corrected using the information obtained from one such check. Bit-flip errors on sites and odd-numbered links require information from two such checks to be corrected. See Table III for the corresponding syndrome outcomes.

sider WLOG an error of the form $X \otimes I \otimes I$ occurring at the level of the underlying phase-flip code. On the logical codespace defined by the basis $|0\rangle_L = (|+++ \rangle + |--- \rangle)/\sqrt{2}$ and $|1\rangle_L = (|+++ \rangle - |--- \rangle)/\sqrt{2}$, this error maps $|0\rangle_L \mapsto |1\rangle_L$. In other words, a physical bit-flip error propagates to a logical bit-flip error which can be detected by our bit-flip correction code. It is easily seen that two bit flip errors leave our code space invariant. The circuit's sensitivity to single qubit phase flip errors propagating to weight two or three phase flip errors from the logical-to-physical CNOT gates is again resolved with the fault-tolerant CNOT construction shown in [Figure 9](#).

Logical bit-flip errors occurring on the logical qubits only propagate to the ancilla qubits and not to the data qubits. The possibility of more than one such error occurring on the data qubits is suppressed by higher powers of p , where p is the probability of an error occurring.

V. DISCUSSION

Error correction involves extending the original Hilbert space of the system to a larger one and endowing the larger Hilbert space with local symmetries that define the codespace. Stabilizers of the codespace are in effect “Gauss’ Law” operators of that symmetry.

We have outlined a simple fault tolerant algorithm which exploits local symmetries to reduce the space requirements for performing error correction on \mathbb{Z}_2 or $U(1)$ LGT systems with a flux cutoff of 1. The logical qubits were concatenated within a phase flip code to attain fault tolerance since phase flip errors commute with the Gauss' Law of these theories.

As we have primarily investigated 1+1 dimensional systems with a flux cutoff of 1, we outline the difficulties one encounters when attempting to generalize these procedures to arbitrary dimensions and flux cutoffs.

For arbitrary flux cutoffs and with non-dynamical matter fields on the sites, the classical CNOT gates in Figure 10 must be replaced with a classically controlled version of the \hat{W}_s operation described in Sec. III B. These are controlled on the state of an appropriate site qubit and can be implemented with adder circuits such as those described in [16, 33]. A fault-tolerant adder will however require non-Clifford operations for a binary integer encoding. In principle, these can be applied using standard techniques like state injection [34] even with our logical encoding. A more scalable solution however is to instead use a unary integer encoding, for which

\mathcal{G}_{2k+1}	\mathcal{G}_{2k}	Error Location
00	00	None
00	11	$ S_{2k}\rangle_L$
11	00	$ S_{2k+1}\rangle_L$
11	11	$ L_{2k+1}\rangle_L$

TABLE III. Table showing how to resolve the ambiguity in the location of a bit-flip error associated to the syndrome 11 for \mathcal{G}_{2k+1} using the syndrome results of \mathcal{G}_{2k} . See Figure 11.

a fault-tolerant incrementer can be implemented using only Clifford gates. The more efficient construction relying on ancilla qubits to compute the XOR between a site and a link variable shown in [Figure 7](#) can also be implemented in a straightforward way when using unary encoding. These will not scale well for large values of the cutoff Λ as the qubit resources will scale linearly with it. However, for a fixed error ε , the cutoff only grows as $\text{polylog}(1/\varepsilon)$ in many physical situations [\[35\]](#).

The scenario with dynamical fermions on the sites is likewise most easily handled by employing a unary encoding on the links. The circuit in [Figure 11](#) then generalizes in the obvious manner, with CNOTs for each qubit in the unary link encoding applied to the proxy qubit $|0\rangle$, and remains fault-tolerant. Generalizations for other types of encodings are less straightforward however and require additional modifications to ensure fault tolerance.

If we consider the case of 2+1 spacetime dimensions, there are four links l connected to each site s and it is always possible to split Gauss' Law to act on two groups of links at a time. This observation applies more generally to arbitrary spacetime dimensions. With larger dimensions however, there are numerous possible choices for the ways the links can be grouped together. While it is expected that the number of Gauss' Law iterations required for error correction should scale independently of the number of lattice points as it is a local symmetry, whether or not certain groupings of links will result in speedups is something that needs further investigation.

Most importantly, we do not claim to encode the full continuous gauge group, as this would violate the fact that finite dimensional quantum systems which correct erasure have no continuous symmetries but only a discrete subgroup thereof [\[36\]](#). As such, we only encode the U(1) symmetry group with a finite cutoff approximation. The construction of error correcting codes analogous to the ones presented here for other structure groups will therefore need to be tailored to their admissible discrete subgroups.

As discussed in Sec. [III B](#), the construction proposed here using an alternating encoding with two qubits per

even link and one qubit per odd link requires $9N$ qubits (excluding ancillas) for the theory with non-dynamical fermions and for pure gauge theory. This improvement in space complexity can also be extended to accommodate dynamical fermions by using Gauss' law to fix errors on the sites and requires $15N$ qubits, excluding ancillas. Such costs cannot be attained from error correcting individual qubits only. The question of whether more efficient encodings could be found by following a more holistic approach as opposed to those using only Gauss' Law on local degrees of freedom (like sites and links) are left for future work. We also point out that when multiple logical qubits are to be encoded, an even lower physical-to-logical qubit ratio is achievable [\[31, 32\]](#).

We make the final observation that the loop string hadron formalism allows the diagonalization of Gauss' law for non-abelian gauge theories, converting them into analogues of those in abelian gauge theories [\[17, 37\]](#). It is expected that this will be an important step in extending these algorithms to more complex theories where additional commuting constraints are needed.

ACKNOWLEDGMENTS

We thank Jesse Stryker and Martin Savage for useful discussions in the early stages of this work. This work was supported in part by the U.S. Department of Energy, Office of Science, Office of Nuclear Physics, Incubator for Quantum Simulation (IQuS) under Award Number DOE (NP) Award DE-SC0020970 and by the DOE QuantISED program through the theory consortium “Intersections of QIS and Theoretical Particle Physics” at Fermilab. It was further supported by a grant from Google research award, and NW’s theoretical work on this project was supported by the U.S. Department of Energy, Office of Science, National Quantum Information Science Research Centers, Co-Design Center for Quantum Advantage under contract number DE-SC0012704.

[1] K. G. Wilson, *Phys. Rev. D* **10**, 2445 (1974).

[2] J. Kogut and L. Susskind, *Phys. Rev. D* **11**, 395 (1975).

[3] J. B. Kogut, *Rev. Mod. Phys.* **51**, 659 (1979).

[4] S. Durr, Z. Fodor, J. Frison, C. Hoelbling, R. Hoffmann, S. D. Katz, S. Krieg, T. Kurth, L. Lellouch, T. Lippert, and et al., *Science* **322**, 1224–1227 (2008).

[5] A. S. Kronfeld, *Annual Review of Nuclear and Particle Science* **62**, 265–284 (2012).

[6] E. Zohar, J. I. Cirac, and B. Reznik, *Reports on Progress in Physics* **79**, 014401 (2015).

[7] M. Dalmonte and S. Montangero, *Contemporary Physics* **57**, 388–412 (2016).

[8] M. C. Bañuls, R. Blatt, J. Catani, A. Celi, J. I. Cirac, M. Dalmonte, L. Fallani, K. Jansen, M. Lewenstein, C. A. Montangero, Simoneand Muschik, B. Reznik, E. Rico, L. Tagliacozzo, K. Van Acocleyen, F. Verstraete, U.-J. Wiese, M. Wingate, J. Zakrzewski, and P. Zoller, *Eur. Phys. J. D* **74**, 165 (2020).

[9] N. Klco, A. Roggero, and M. J. Savage, “Standard model physics and the digital quantum revolution: Thoughts about the interface,” (2021), [arXiv:2107.04769 \[quant-ph\]](#).

[10] J. C. Halimeh and P. Hauke, *Phys. Rev. Lett.* **125**, 030503 (2020).

[11] P. Hauke, D. Marcos, M. Dalmonte, and P. Zoller, *Phys. Rev. X* **3**, 041018 (2013).

[12] M. V. Damme, J. C. Halimeh, and P. Hauke, “Gauge-symmetry violation quantum phase transition in lat-

tice gauge theories,” (2020), arXiv:2010.07338 [cond-mat.quant-gas].

[13] A. Rajput, A. Roggero, and N. Wiebe, “Hybridized methods for quantum simulation in the interaction picture,” (2021), arXiv:2109.03308 [quant-ph].

[14] H. Lamm, S. Lawrence, and Y. Yamauchi, “Suppressing coherent gauge drift in quantum simulations,” (2020), arXiv:2005.12688 [quant-ph].

[15] M. C. Tran, Y. Su, D. Carney, and J. M. Taylor, *PRX Quantum* **2**, 010323 (2021).

[16] J. R. Stryker, *Physical Review A* **99** (2019), 10.1103/physreva.99.042301.

[17] I. Raychowdhury and J. R. Stryker, *Phys. Rev. Research* **2**, 033039 (2020).

[18] N. Klco and M. J. Savage, “Hierarchical qubit maps and hierarchical quantum error correction,” (2021), arXiv:2109.01953 [quant-ph].

[19] P. W. Shor, *Phys. Rev. A* **52**, R2493 (1995).

[20] R. Chao and B. W. Reichardt, *Physical Review Letters* **121** (2018), 10.1103/physrevlett.121.050502.

[21] D. P. DiVincenzo and P. W. Shor, *Phys. Rev. Lett.* **77**, 3260 (1996).

[22] R. Laflamme, C. Miquel, J. P. Paz, and W. H. Zurek, *Phys. Rev. Lett.* **77**, 198 (1996).

[23] J. Schwinger, *Phys. Rev.* **128**, 2425 (1962).

[24] S. Coleman, R. Jackiw, and L. Susskind, *Annals of Physics* **93**, 267 (1975).

[25] M. Bañuls, K. Cichy, J. Cirac, and K. Jansen, *Journal of High Energy Physics* **2013** (2013), 10.1007/jhep11(2013)158.

[26] T. Pichler, M. Dalmonte, E. Rico, P. Zoller, and S. Montangero, *Phys. Rev. X* **6**, 011023 (2016).

[27] E. A. Martinez, C. A. Muschik, P. Schindler, D. Nigg, A. Erhard, M. Heyl, P. Hauke, M. Dalmonte, T. Monz, P. Zoller, and et al., *Nature* **534**, 516–519 (2016).

[28] N. Klco, E. F. Dumitrescu, A. J. McCaskey, T. D. Morris, R. C. Pooser, M. Sanz, E. Solano, P. Lougovski, and M. J. Savage, *Phys. Rev. A* **98**, 032331 (2018).

[29] M. A. Nielsen and I. L. Chuang, *Quantum Computation and Quantum Information: 10th Anniversary Edition*, 10th ed. (Cambridge University Press, USA, 2011).

[30] A. Córcoles, E. Magesan, S. J. Srinivasan, A. W. Cross, M. Steffen, J. M. Gambetta, and J. M. Chow, *Nat. Comm.* **6**, 6979 (2015).

[31] D. Gottesman, *Phys. Rev. A* **54**, 1862 (1996).

[32] A. R. Calderbank, E. M. Rains, P. W. Shor, and N. J. A. Sloane, *Phys. Rev. Lett.* **78**, 405 (1997).

[33] A. F. Shaw, P. Lougovski, J. R. Stryker, and N. Wiebe, *Quantum* **4**, 306 (2020).

[34] S. Bravyi and J. Haah, *Physical Review A* **86** (2012), 10.1103/physreva.86.052329.

[35] Y. Tong, V. V. Albert, J. R. McClean, J. Preskill, and Y. Su, “Provably accurate simulation of gauge theories and bosonic systems,” (2021), arXiv:2110.06942 [quant-ph].

[36] P. Faist, S. Nezami, V. V. Albert, G. Salton, F. Pastawski, P. Hayden, and J. Preskill, *Physical Review X* **10** (2020), 10.1103/physrevx.10.041018.

[37] Z. Davoudi, I. Raychowdhury, and A. Shaw, *Phys. Rev. D* **104**, 074505 (2021).